

An upwind finite difference scheme for singularly perturbed parabolic convection-diffusion with discontinuous initial conditions on piecewise-uniform mesh

Desto Sodano Sheiso^a

Email addresses: desto.sodano@iitg.ac.in (Desto Sodano Sheiso), destasodano2010@gmail.com (Desto Sodano Sheiso)

^aDepartment Of Mathematics, Indian Institute Of Technology Guwahati, Guwahati - 781 039, India

Abstract

This article presents the numerical approximations for solve singularly perturbed parabolic convection-diffusion problems (SPPCDP) with discontinuous initial conditions. The scheme uses backward- Euler for temporal derivatives on a uniform mesh and classical upwind finite difference for spatial derivatives on a piecewise-uniform (Shishkin) mesh. This scheme provides almost a first-order convergence solution in space and time variables. The method employs an upwind finite difference operator on a piecewise-uniform mesh to approximate the gap between the analytic function and the parabolic issue solution. Through comprehensive analysis, we explore the stability and accuracy of the proposed scheme, considering its efficacy in addressing challenges posed by singular perturbations and abrupt changes in the solution. The results provide valuable insights into the applicability of the approach for convection-dominated problems with complex initial conditions, contributing to the advancement of numerical methods in this domain. Parameter-uniform error estimates, stability results, and bounds for the truncation errors are all addressed. Finally, numerical experiments are presented to validate our theoretical results.

Keywords: Singularly perturbed parabolic convection-diffusion problems, Upwind finite difference scheme, piecewise-uniform mesh

Subject Classifications: AMS 65M06, 65M12, 65M15.

Date of Submission: 09-09-2023

Date of Acceptance: 19-02-2024

I. Introduction

This article will delve into a particular type of problem called SPPCDPs, which exhibit interior layers caused by discontinuous initial conditions [1, 16, 22]. These concerns are pertinent across various engineering and applied mathematical domains, including convection-dominated flows in fluid dynamics, quantum mechanics, elasticity, chemical reactor theory, gas porous electrodes theory, as well as heat and mass transfer in chemical and nuclear engineering. Our investigation is rooted in the studies conducted by Gracia *et al.* [12] and [13] in the field of numerical analysis. The paper introduces an analytical function that aligns with discontinuous initial conditions and solves a differential equation with constant coefficients. The interior layer function's position evolves over time in the convection-diffusion problem, requiring tracking techniques like the Shishkin mesh. An explicit discontinuous function $S(x, t)$ captures the discontinuous initial conditions-related singularity, and asymptotic expansions for the solution $u(x, t)$ are constructed. Subtracting this singular function yields $y(x, t) = u(x, t) - S(x, t)$, the solution of an SPCDP. In [5, 14, 15], studied singularly perturbed reaction-diffusion problems in which discontinuities existed in either the boundary or the initial condition. Here, we expand this approach to address a convection-diffusion problem with discontinuous initial conditions. This introduces a time-dependent shift in the position of the interior layer arising from the initial condition discontinuity. These types of problems arise in several branches of engineering and applied mathematics, including convection-dominated flows in fluid dynamics, quantum mechanics, elasticity, chemical reactor theory, gas porous electrodes theory, heat, and mass transfer in chemical and nuclear engineering, etc.[9, 10]. In [15], we introduce an alternative numerical algorithm that incorporates a coordinate transformation designed to align the mesh with the interior layer location, allowing us to handle this more general case effectively. The linearized Navier-Stokes equations at high Reynolds numbers, heat transport problems with large Péclet numbers, and magneto-hydrodynamic duct problems at Hartman numbers are well-known examples of singularly perturbed problems (SPPs) [19, 10, 9, 24].

Classical numerical methods, as acknowledged in [19, 20, 24, 10], prove ineffective in approximating solutions of SPPs. Moreover, as ε approaches zero, standard finite difference or finite element schemes on uniform meshes fall short in handling singularly perturbed differential equations (SPDE) with continuous data. As evident from the literature cited above, most researchers aim to discover a numerical solution for SPPCDP. However, this paper introduces a novel approach by developing and evaluating parameter-uniform numerical techniques, utilizing piecewise-uniform meshes, specifically designed for a class of SPPCDP with discontinuous initial conditions. Therefore, developing parameter-uniform numerical methods is a well-established principle in the study of numerical solutions to SPPs.

Several researchers, such as Clavero et al. [5, 4, 21], Kopteva [14], and Shishkin [5, 26], have developed algorithms for SPPCDP with uniform second-order convergence in both variables. The problem involves initial conditions with discontinuities, resulting in interior and boundary layers. For parabolic problems, the initial layer's location evolves over time in convection-diffusion scenarios but remains fixed in reaction-diffusion cases. The interior layer moves along a characteristic curve related to the reduced problem in the considered model. Gracia and O'Riordan [13, 14, 15] have investigated the interior layer's movement in convection-diffusion SPPs, while Shishkin [1, 25] studied parabolic SPPs with piecewise smooth initial data using finite difference grids. Gracia and O'Riordan [15, 11, 23] established a parameter-uniform numerical method for problems with incompatible boundary and initial data. Numerous authors have utilized this technique to enhance convergence order, albeit at increased computational complexity [17]. O'Riordan *et al.* [7] combined implicit Euler with the classical upwind finite difference operator on a piecewise uniform mesh in one dimension, achieving first-order parameter-uniform convergence in both space and time variables.

Academic publications show a technique achieving higher-order convergence compared to classical numerical schemes for singularly perturbed convection-diffusion problems using Shishkin meshes, extensively explored by Gracia and Clavero as evidenced by citations like [12, 24, 25, 26]. Shishkin *et al.* [25] developed parameter-uniform numerical methods for singularly perturbed parabolic problems with discontinuous initial condition terms, using fitted operator techniques instead of upwind finite difference operators.

The focus of this study is on the development and analysis of an upwind finite difference scheme tailored specifically for such singularly perturbed parabolic convection-diffusion problems. The challenges addressed in this research are rooted in the complexity of real-world scenarios where initial conditions exhibit abrupt changes, a common occurrence in practical applications. The utilization of a piecewise-uniform grid provides a practical framework for discretizing spatial domains, offering adaptability to capture localized variations [3, 1].

By delving into the numerical intricacies of convection-dominated problems with discontinuous initial conditions, this research aims to contribute to the advancement of computational methods applicable to real-world situations. The outcomes of this study are expected to have direct implications for industries and research areas where accurate predictions and simulations are crucial for informed decision-making and enhanced understanding of complex physical processes [6].

In this paper, we look at a group of SPPCDPs that generate solutions with internal layers as a result of discontinuous initial conditions. Existing literature proposes various methods to address these issues. To gain a comprehensive understanding of these techniques, we recommend consulting the book by Farrell *et al.*'s [9, 10] and R  os *et al.*'s work [24]. M. Pickett and G. Shishkin [26] employed parameter-uniform finite differences to solve singularly perturbed parabolic diffusion-convection-reaction problems. For a more in-depth exploration of numerical treatments of SPPs, reference the works cited in [19, 20], including works by Clavero, Miller, and Shishkin [4, 2, 5], Farrell, Hegarty, Miller, O'Riordan, and Shishkin, Roos, Stynes, and Tobiska [10, 19, 20]. The article divides numerical methods for SPPs into two categories: fitted operator methods using exponentially fitted finite difference schemes on uniform meshes (Doolan et al. [18]), and fitted mesh methods using classical finite difference schemes on non-uniform grids (Farrell, Hegarty, Miller, O'Riordan, and Shishkin [19, 20], Roos, Stynes, and Tobiska [24]).

With this motivation, our goal is to solve SPPCDP with discontinuous initial conditions using first-order finite difference schemes over piecewise-uniform mesh and to improve the accuracy of numerical solutions for one-dimensional SPPCDP with discontinuous initial conditions (2.1). We want to enhance the order of accuracy for SPPs [17] basic upwind finite difference techniques. The asymptotic expansion technique will be used to provide exact constraints for the continuous solution and its derivatives. We will also look at how this strategy can improve the order of accuracy for basic upwind finite difference schemes in the SPP class with discontinuous initial conditions. This method proves highly beneficial in approximating both temporal and spatial derivatives. We can enhance the convergence of the implicit

upwind finite difference method.

The rest of the article is organized as follows: Section 2 defines a continuous problem using a transformation to fix the interior layer's position in time, providing solution decomposition, derivatives, and discontinuous initial conditions-defined singular function. Section 3 introduces a numerical scheme in the transformed domain based on a classical implicit upwind scheme and establishes a parameter-uniform error bound. Section 4 we present numerical examples to validate the theoretical results. The paper concludes with the conclusions.

Notations In this paper, C is a constant independent of both the singular perturbation parameter ε and all discretization parameters. The jump of a function ϕ at a discontinuity point \tilde{d} is defined as:

$$[\phi](\tilde{d}) = \phi(\tilde{d}^+) - \phi(\tilde{d}^-).$$

We denote the maximum norm over any region $\|\cdot\|_{\tilde{D}}$, which is defined by $\|u\|_{\tilde{D}} = \max_{x \in \tilde{D}} |u(x, t)|$, $(x, t) \in D$ for any function u .

II. Statement of the solution

In this paper, we consider the following SPCCDP with the discontinuous initial conditions defined on domain D :

$$\begin{cases} L_\varepsilon u = u_t - \varepsilon u_{xx} + a(x, t)u_x + b(x, t)u = f(x, t), (x, t) \in D, \\ u(x, 0) = \phi(x), 0 \leq \tilde{d} \leq 1; [\phi](\tilde{d}) \neq 0, 0 \leq \tilde{d} \leq 1; \\ u(0, t) = u(1, t) = 0, \quad 0 < t \leq T \end{cases} \quad (2.1)$$

where $D = \Omega \times (0, T]$, $\Omega = (0, 1)$, $t \in (0, T]$, $T > 0$, and $0 < \varepsilon \ll 1$ is a singular perturbation parameter and the coefficients $a(x, t)$, $b(x, t)$ are smooth and satisfy $a(x, t) > \alpha > 0$, $b(x, t) \geq \beta \geq 0$ on Ω .

We assume that the functions a, f, ϕ satisfy the below conditions:

$$a, f \in C^{4+\gamma}(D) \text{ for some } \gamma > 0, \text{ and } \phi^{(i)}(0) = \phi^{(i)}(1) = 0, \quad 0 \leq i \leq 4.$$

Moreover, $[\phi]$ denotes the jump in the function ϕ across the point of discontinuity $x = \tilde{d}$, that is, $[\phi](\tilde{d}) = \phi(\tilde{d}^+) - \phi(\tilde{d}^-)$.

In general, due to the presence of a discontinuity in the convection coefficient $a(x)$, the solution $u(x, t)$ of the problem (2.1) possesses an interior layer in the neighborhood of the point $x = \tilde{d}$. We observe that the initial function $\phi(x)$ is discontinuous at $x = \tilde{d}$ and the location of this point does not depend on the singular perturbation parameter ε . The initial condition ϕ is smooth, but it contains the interior layer in the vicinity of the layer $x = \tilde{d}$. We assume that the initial data ϕ and f are sufficiently smooth functions on the domain \tilde{D} [18, 30] and that satisfy sufficient compatibility conditions at the corner points $(0, 0)$ and $(1, 0)$. We also assume that the required compatibility conditions at the transition point $(\tilde{d}, 0)$ follow a similar pattern.

Assuming sufficient smoothness and compatibility conditions on ϕ and f , the parabolic problem (2.1) typically has a unique solution $u(x, t)$. This solution displays a regular boundary layer of width $O(\varepsilon)$ at $x = 1$. Additionally, in the range $a(t) > \alpha > 0$, $0 \leq t \leq T$, $a, f \in C^{4+\gamma}(D)$, we presume that b and f constitute suitably regular layer components. Moreover, we assume adequate compatibility at the points $(0, 0)$ and $(1, 0)$ to ensure $u \in C^{4+\gamma}(D)$. Given $\alpha > 0$, the function $\tilde{d}(t)$ exhibits monotonically increasing behavior. We assume that the convection term $a(x, t)$ is dependent on both the time and space and so the location of the interior layer does not remain at the same position throughout the process. Thus, we need to track the movement of the layer.

The discontinuity in the initial condition generates an interior layer emanating from the point $(\tilde{d}, 0)$. By identifying the leading term $\frac{1}{2}[\phi]\tilde{d}^{-\varphi_0}$ in an asymptotic expansion of the solution, we can define the following continuous function

$$y(x, t) = u(x, t) - S(x, t) \quad (2.2)$$

Where $S(x, t) = \frac{1}{2}[\phi]\tilde{d}^{-\varphi_0}(x, t)$, $\varphi_0(x, t) = \text{erf}\left(\frac{\tilde{d}(t)-x}{\sqrt{2\varepsilon t}}\right)$, $\text{erfc}(z) = \frac{2}{\sqrt{\pi}} \int_z^\infty e^{-r^2} dr$ with $L_\varepsilon = f + \frac{1}{2}[\phi]\tilde{d}^{-\varphi_0}(a(\tilde{d}(t)) - t - a(x, t)) \mp \varphi_0(x, t)$.

The function y satisfies the following problem:

$$\begin{cases} L_\varepsilon y = 0, (x, t) \in D, \\ y(x, 0) = \frac{1}{2}[\phi]\tilde{d}^{-\varphi_0}(x, t); 0 < t \leq T \\ y(1, t) = \frac{1}{2}[\phi]\tilde{d}^{-\varphi_0}(x, t), \quad 0 < t \leq T, y(x, 0) = [\phi], x < \tilde{d}^+ \quad y(x, 0) = [\phi](\tilde{d}^-), x = \tilde{d}^+ \quad y(x, 0) = \phi(x) - [\phi](\tilde{d}), x > \tilde{d}^+ \end{cases} \quad (2.3)$$

Applications of transformation to fix interior layer

One possible choice for the transformation $X : (x, t) \rightarrow (v, t)$ is the piecewise linear map given by

$$v(x, t) = \begin{cases} \frac{\tilde{d}}{d(t)}x, & x \leq \tilde{d}(t) \\ 1 - \frac{1 - \tilde{d}}{1 - d(t)}(1 - x), & x \geq \tilde{d}(t) \end{cases} \quad (2.4)$$

which means that $a(\tilde{d}(t), t) = a(\tilde{d}, t)$.

Applying this mapping for numerical solutions transforms (2.1) into the problem of finding y . Consequently, the transformed equation takes the form:

$$\begin{cases} L_\varepsilon y = g \left(f + \frac{1}{2} [\phi](\tilde{d}) \frac{(a(\tilde{d}(t) - t - a(k, t)) e^{-g(k, t)(k - \tilde{d})^2}}{\sqrt{\varepsilon \pi t}} \right), x \neq \tilde{d}, \\ [y](\tilde{d}, t) = 0 \\ [\frac{1}{\sqrt{g}} y_x](\tilde{d}, t) = 0. \end{cases} \quad (2.5)$$

Decomposition of the solution

To develop sharp bounds in the error analysis, we decompose the solution $y(x, t)$ of (2.5) into the sum of smooth layer component $p(x, t)$, singular layer component $q(x, t)$ and the interior layer component $z(x, t)$ as follows:

$$y(x, t) = p(x, t) + q(x, t) + \frac{1}{2} \sum_{i=2}^4 [\phi^{(i)}](\tilde{d}) \frac{(-1)^i}{i!} \varphi + z(x, t), \quad p, q \in C^{4+\gamma}(D).$$

The smooth component $p(x, t)$ is represented using an asymptotic expansion:

$$p(x, t) = \sum_{i=0}^3 \varepsilon^i p_i(x, t), \quad (x, t) \in \bar{D}.$$

III. Numerical methods

This section uses backward-Euler and central differences on a piecewise-uniform Shishkin mesh to approximate (2.3). We then discretize the SPPCDP with discontinuous initial conditions (2.1) using backward-Euler for time and upwind finite differences for space, achieving ε -uniform convergence.

Construction of piecewise-uniform Shishkin mesh

Assuming that N and $M = O(N)$ are both positive integers, we consider the domain $D^- = \Omega^- \times [0, T] = [0, 1] \times [0, T]$. Additionally, let $N \geq 4$ be a positive even integer. We construct a piecewise uniform Shishkin mesh to handle the boundary layer at $x = 1$ in the SPPCDP with DIC (2.1). We establish the uniform temporal mesh as follows:

$$\hat{\Omega}_t^M = \{t_k : t_k = k\Delta t, k = 0, \dots, M, t_0 = 0, t_M = T, \Delta t = T/M\},$$

where M is the number of mesh elements in the time direction, and step sizes k .

where M is the number of mesh elements in the time direction, and step sizes k . Let's denote the spatial mesh widths as $h_i = x_i - x_{i-1}$ and $\hat{h} = h_i - h_{i+1}$ for $i = 1, \dots, N - 1$. We divide the transformed spatial domain $\Omega = [0, 1]$ into the following four sub-intervals as follows:

$$\Omega = [0, \tilde{d} - \tau_1] \cup [\tilde{d} - \tau_1, \tilde{d}] \cup [\tilde{d} + \tau_2, 1 - \hat{\tau}_x] \cup [1 - \hat{\tau}_x, 1].$$

For the spatial mesh with N grids, the transition points τ_1, τ_2 and $\hat{\tau}_x$ are defined by

$$\begin{cases} \hat{\tau}_x = \min \left\{ \frac{1}{4}, 2\sqrt{\varepsilon/\alpha \ln N} \right\}, \\ \tau_1 = \min \left\{ \frac{\tilde{d} - \hat{\tau}_x}{4}, 2\sqrt{T\varepsilon \ln N} \right\}, \\ \tau_2 = \min \left\{ 1 - \tilde{d}(T), \frac{\tilde{d} - \hat{\tau}_x}{4}, 2\sqrt{T\varepsilon/\delta \ln N} \right\}. \end{cases} \quad (3.1)$$

The mesh interval point N of spatial grids are distributed into four intervals in the ratio $3N/8 : N/4 : N/4 : N/8$ and each of them is spaced uniformly. The spatial and temporal domains are denoted by $\hat{\Omega}_x^N$ and $\hat{\Omega}_t^M$ respectively. Thus, the discretized computational domain $\bar{D}^{N,M}$ is defined as $\bar{D}^{N,M} = \hat{\Omega}_x^N \times \hat{\Omega}_t^M, \partial D^{N,M} = \bar{D}^{N,M} \setminus D^{N,M}$.

Numerical scheme in the transformed domain and classical implicit upwind finite difference scheme

For any discrete function $v_i^n \approx v(x_i, t_n)$, we define the first-order forward D_x^+ , backward D_x^- , central D_x^0 difference operators, the backward finite difference operator D_t^- in time which is given in appendix section.

We discretize the transformed problem (2.5) and use the backward-Euler method for the time derivative and upwind finite difference scheme to approximate spatial derivatives. The discrete problem can be defined by the

following: Find Y such that

$$\left\{ \begin{array}{l} L_{\varepsilon}^{N,M} Y^{N,\Delta t}(x_i, t_j) = f(x_i, t_j) = (D_x^- - \varepsilon \delta_x^2 + a D_x^- + b I) Y^{N,\Delta t}(x_i, t_j), (x_i, t_j) \in D^{N,M}, x_i \neq \tilde{d} \\ L_{\varepsilon}^{N,M} Y^{N,\Delta t}(x_i, t_j) \\ \left[\frac{1}{\sqrt{g}} D_x^c \right] (\tilde{d}, t_j) = 0, x_i = \tilde{d}, t_j > 0, \\ Y_{ij} = (x_i, t_j) \in \partial \bar{D}^{N,M}, \\ Y(0, t) = Y(1, t) = 0, t \geq 0, \end{array} \right. \quad (3.2)$$

Theorem 3.3.

For large enough N and M = O(N). If Y is the solution of the discrete problem (3.2) and y is the solution of (2.5), then the global approximation of \bar{Y} on $\bar{D}^{N,M}$ and bilinear interpolation and the error associated with the discrete solution $Y^{N,\Delta t}$ at time level t_n is given by satisfies

$$|y(x_i, t_n) - \bar{Y}^{N,\Delta t}(x_i, t_n)| \leq C(N^{-1} \ln N + \Delta t), (x_i, t_n) \in D^{N,M}, 1 \leq i \leq N - 1.$$

Proof. The detailed proof is given in [8, 28]

IV. Numerical Examples, Results and Discussion

In this section, we validate theoretical results by applying a classical upwind finite difference scheme to a test problem. We conduct numerical tests to affirm theoretical findings, employing model problems from equations (2.1) and utilizing the numerical scheme outlined in equations (3.2). This section showcases three examples. Given that exact solutions are unknown, we evaluate the maximum point-wise error utilizing the double mesh principle [15, 13].

Let $\bar{Y}^{N,M}$ denote the bilinear interpolation of the discrete solution Y N,M on the piecewise-uniform Shishkin mesh $\bar{D}^{N,M}$. Then, the maximum point-wise of the double mesh principle of global difference is given by

$$E_{\varepsilon}^{N,M} = \|\bar{Y}^{N,M}(x_i, t_n) - \bar{Y}^{2N,2M}(x_i, t_n)\|.$$

Also, the ε -uniform maximum point-wise error $E^{N,M}$ and the corresponding ε -uniform order of convergence $P^{N,M}$ is given by $E^{N,M} = \max_{\varepsilon} E_{\varepsilon}^{N,M}$, $P^{N,M} = \log_2 \left(\frac{E_{\varepsilon}^{N,M}}{E_{\varepsilon/2}^{2N,2M}} \right)$.

For each value of N satisfying $N, 2N \in R_N = [32, 64, 128, 256, 512, 1024, 2048]$, we calculate the ε -uniform maximum pointwise double-mesh differences $E^{N,M}$. In our experiments, we examine the parameter set $\varepsilon = 2^0, \dots, 2^{-18}$. We calculate solutions $Y^{N,M}$ and $Y^{2N,2M}$ using (3.2) on piecewise-uniform Shishkin meshes $\bar{E}^{N,M}$ and $\bar{E}^{2N,2M}$ with $N = M = 64$. For all three test examples, we provide plots of $\bar{Y}^{N,M}$ and $\bar{U}^{N,M} = \bar{Y}^{N,M} + \bar{S}$ for $\varepsilon = 2^{-12}$ and $N = M = 64$.

The interior layers do not interact with the boundary layer in the first two examples and in the third example, the interior layer does interact with the boundary layers.

Classical upwind finite difference scheme

We summarize the outcomes of our numerical experiments involving discontinuous initial data in this case.

The performed MATLAB computation is based on the following:

- 1. **Numerical scheme.** Classical upwind scheme in space and backward-Euler scheme in time.
- 2. **Mesh Structure:** Shishkin mesh.

In this example, the final time has been selected to be sufficiently large, so that the interior layer interacts with the boundary layer.

In the first and second examples, the interior layer does not interact with the boundary layer. But, in the third example, the interior layer interacts with the boundary layer. Figure 1, 2, and 3 shows computed approximations for Y and the numerical solution U with the scheme (3.2) and presents a surface plot of

the numerical solution with $N = M = 64$ and $\varepsilon = 2^{-12}$. Unlike Example 1, where $[\phi](0.3) \neq 0$, here the influence of the initial condition on the convergence order is apparent. The order is reduced to 0.5, aligning with the error bound from Theorem 3.3. Tables display uniform double mesh global differences, demonstrating almost first-order convergence when approximating component \tilde{d} . The results presented in the tables provide support for the theoretical error estimates outlined in Theorem 3.3.

To solve the SPPCDP in Examples 4.1, 4.2, and 4.3, we employ the upwind finite difference method for spatial derivatives and the implicit-Euler strategy for temporal derivatives on two meshes ($E^{N,M}$ and $E^{2N,2M}$). Here, the data provided that by using upwind finite difference scheme table 1, 2, and 3 presents the maximum error and order of convergence, then we obtain almost first-order convergence

rate.

Example 4.1. Consider the following singularly perturbed parabolic problem:

$$\begin{cases} -\varepsilon u_{xx} + x(1+t^2)u_x + u_t = 4x(1-x)t + t^2, & (x,t) \in (0,1) \times (0,1/2), \\ u(x,0) = -2, & 0 \leq x < \tilde{\square}; u(x,0) = 1, & \tilde{\square} \leq t \leq 1, \\ u(0,t) = -2, u(1,t) = 1, & 0 < t \leq 0.5 \end{cases} \quad (5.1)$$

The discontinuous initial condition is given by

where $\tilde{\square} = 0.3$, $T = 0.5$ and $\alpha = 1$.

Example 4.2. Consider the following singularly perturbed parabolic problem:

$$\begin{cases} -\varepsilon u_{xx} + x(1+t)u_x + u_t = 4x(1-x)t + t^2, & (x,t) \in (0,1) \times (0,1/2), \\ u(x,0) = -x^3, & 0 \leq x < \tilde{\square}; u(x,0) = (1-x)^3, & \tilde{\square} \leq t \leq 1, \\ u(0,t) = 0, u(1,t) = 0, & 0 < t \leq 0.5 \end{cases} \quad (5.2)$$

The discontinuous initial condition is given by

where $\tilde{\square} = 0.3$, $T = 2$ and $\alpha = 1$.

Example 4.3. Consider the following singularly perturbed parabolic problem:

$$\begin{cases} -\varepsilon u_{xx} + x(1+t)u_x + u_t = 4x(1-x)t + t^2, & (x,t) \in (0,1) \times (0,1/2), \\ u(x,0) = -2, & 0 \leq x < \tilde{\square}; u(x,0) = 1, & \tilde{\square} \leq t \leq 1, \\ u(0,t) = -2, u(1,t) = 1, & 0 < t \leq 0.5 \end{cases} \quad (5.3)$$

The discontinuous initial condition is given by

where $\tilde{\square} = 0.3$, $T = 0.5$ and $\alpha = 1$.

The characteristic curve $\tilde{\square} = t^{1/2} / 2 + 0.3$.

In this example, the final time has been selected to be sufficiently large, so that the interior layer interacts with the boundary layer.

In the first and second examples, the interior layer does not interact with the boundary layer. But, in the third example, the interior layer interacts with the boundary layer. Figure 1, 2, and 3 shows computed approximations for Y and the numerical solution U with the scheme (3.2) and presents a surface plot of the numerical solution with $N = M = 64$ and $\varepsilon = 2^{-12}$. Unlike Example 1, where $[\phi'](0.3) \neq 0$, here the influence of the initial condition on the convergence order is apparent. The order is reduced to 0.5, aligning with the error bound from Theorem 3.3. Tables display uniform double mesh global differences, demonstrating almost first-order convergence when approximating component $\tilde{\square}$. The results presented in the tables provide support for the theoretical error estimates outlined in Theorem 3.3.

V. Conclusions

This article examines the use of first-order upwind finite difference schemes to solve SPPCDPs with discontinuous initial conditions (2.1). First, we use the piecewise-uniform Shishkin mesh to discretize the domain, and then we use implicit Euler for time discretization on a uniform mesh and an upwind finite difference method for spatial discretization. The results show almost first-order convergence for the upwind finite difference schemes. The technique achieves ε -uniform convergence with first-order accuracy with a modest logarithmic computational component. Tables 1, 2, and 3 offer precise estimates of maximum pointwise errors and convergence rates for Examples 4.1, 4.2, and 4.3, indicating almost first-order convergence. The numerical experiments on three test problems validate the theoretical findings.

Table 1: Maximum point-wise errors and the corresponding order of convergence for the function y in Example 4.1, computed using the upwind scheme.

ϵ	Number of Mesh Intervals ($N = M$)					
	32	64	128	256	512	1024
	1.088	1.048	1.024	1.012	1.006	3.396e-04
2^{-3}	1.673e-02 0.633	1.079e-02 1.055	5.191e-03 1.027	2.547e-03 1.013	1.262e-03 1.007	6.280e-04
2^{-4}	2.008e-02 0.776	7.991e-03 0.781	4.652e-03 0.816	2.642e-03 0.832	1.484e-03 0.850	8.235e-04
2^{-6}	4.800e-03 0.831	2.698e-03 0.792	1.557e-03 0.813	8.862e-04 0.833	4.976e-04 0.848	2.763e-04
2^{-8}	2.468e-03 0.900	1.323e-03 0.866	7.255e-04 0.862	3.993e-04 0.857	2.204e-04 0.851	1.221e-04
2^{-10}	2.875e-03 0.776	1.679e-03 0.841	9.370e-04 0.854	5.184e-04 0.858	2.860e-04 0.864	1.572e-04
2^{-12}	2.968e-03 0.798	1.707e-03 0.839	9.543e-04 0.852	5.288e-04 0.853	2.927e-04 0.861	1.612e-04
2^{-14}	2.992e-03 0.804	1.714e-03 0.839	9.586e-04 0.851	5.313e-04 0.852	2.943e-04 0.859	1.623e-04
....
2^{-18}	1.368e-03 0.736	4.806e-03 0.760	2.838e-04 0.798	1.632e-04 0.815	9.278e-04 0.820	5.255e-04
$E^{N,M}$	2.008e-02	1.079e-02	5.191e-03	2.642e-03	1.484e-03	8.235e-04
$P^{N,M}$	0.896	1.055	0.974	0.832	0.849	

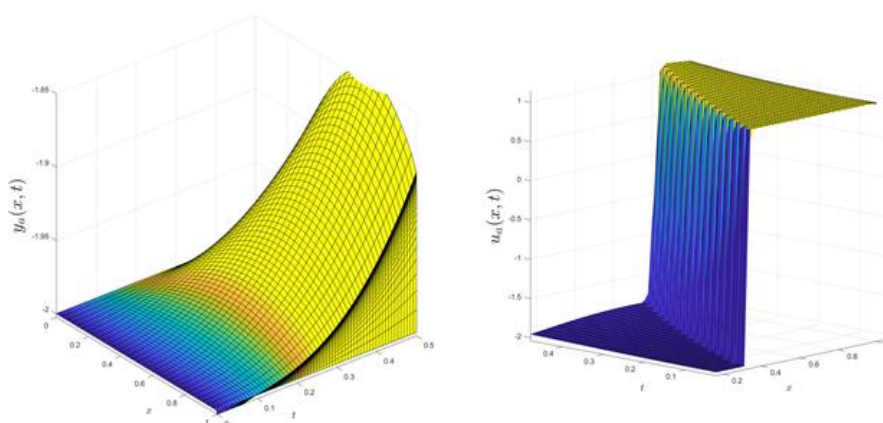


Figure 1: Surface plot of numerical approximation to y and u with $\epsilon = 2^{-12}$ and $N = M = 64$ for Example 4.1.

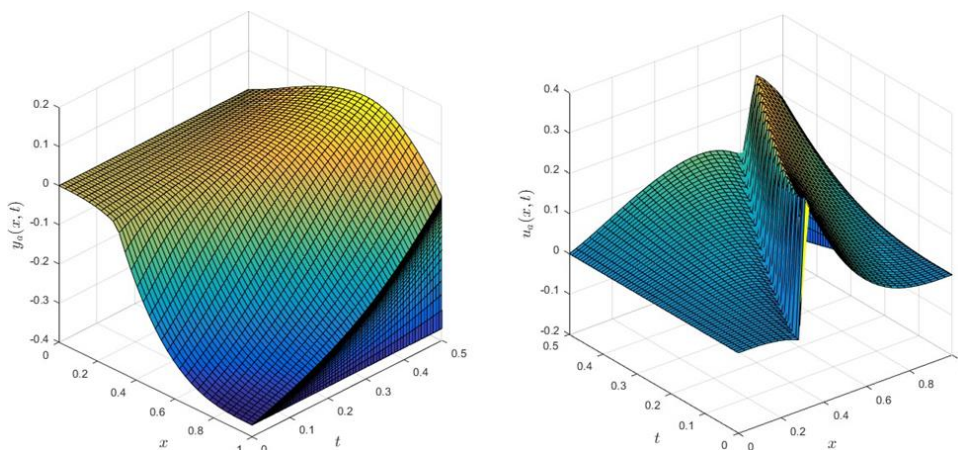


Figure 2: Surface plot of numerical approximation to y and u with $\varepsilon = 2^{-12}$ and $N = M = 64$ for Example 4.2.

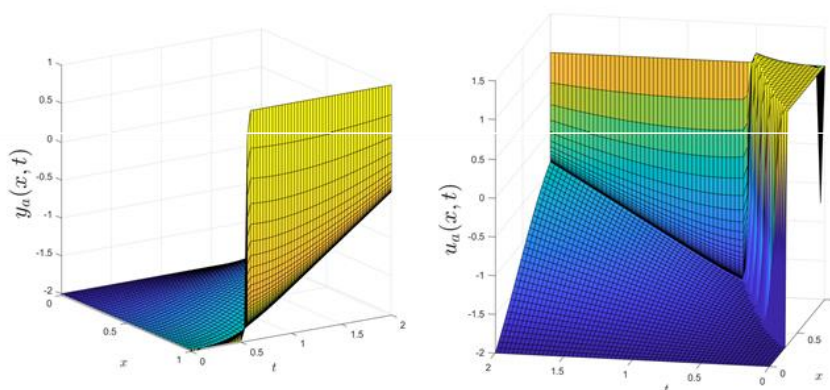


Figure 3: Surface plot of numerical approximation to y and u with $\varepsilon = 2^{-12}$ and $N = M = 64$ for Example 4.3.

Table 2: Maximum point-wise errors and the corresponding order of convergence for the function y in Example 4.2, computed using the upwind scheme.

ε	Number of Mesh Intervals ($N = M$)					
	32	64	128	256	512	1024
	-0.348	0.603	0.278	0.550	0.367	1.314e-03
2^{-4}	7.415e-03 0.894	3.990e-03 0.823	2.255e-03 0.854	1.247e-03 0.656	7.917e-04 0.259	6.614e-04
2^{-6}	1.125e-02 0.674	7.051e-03 0.796	4.061e-03 0.883	2.202e-03 0.933	1.154e-03 0.969	5.894e-04
2^{-8}	1.425e-02 0.551	9.726e-03 0.610	6.373e-03 0.701	3.921e-03 0.784	2.277e-03 0.8671	1.248e-03
2^{-10}	1.519e-02 0.482	1.088e-02 0.524	7.564e-03 0.558	5.138e-03 0.620	3.344e-03 0.697	2.063e-03
2^{-12}	1.543e-02 0.461	1.121e-02 0.497	7.945e-03 0.495	5.636e-03 0.527	3.911e-03 0.561	2.651e-03
2^{-14}	1.550e-02 0.456	1.130e-02 0.490	8.048e-03 0.478	5.777e-03 0.494	4.102e-03 0.504	2.893e-03
....
2^{-18}	1.421e-02 0.736	4.806e-02 0.760	2.838e-03 0.798	1.632e-03 0.815	9.278e-03 0.820	5.255e-03

$E^{N,M}$	1.550e-02	1.130e-02	8.048e-03	5.777e-03	4.102e-03	2.893e-03
$P^{N,M}$	0.455	0.489	0.478	0.494	0.503	

Table 3: Maximum point-wise errors and the corresponding order of convergence for the function y in Example 4.3, computed using the upwind scheme.

ϵ	Number of Mesh Intervals ($N = M$)					
	32	64	128	256	512	1024
	0.963	0.981	0.990	0.995	0.997	1.594e-03
2^{-3}	7.498e-02 0.511	5.263e-02 0.975	2.677e-02 0.988	1.350e-02 0.993	6.782e-03 0.996	3.399e-03
2^{-4}	7.313e-02 0.630	4.724e-02 0.749	2.811e-02 0.751	1.670e-02 0.802	9.579e-03 0.824	5.411e-03
2^{-6}	6.547e-02 0.987	3.302e-02 0.582	2.205e-02 0.663	1.392e-02 0.708	1.154e-03 0.782	3.363e-03
2^{-8}	7.872e-02 0.769	4.619e-02 0.758	2.731e-02 0.753	1.621e-02 0.801	9.305e-03 0.819	5.274e-03
2^{-10}	6.44e-02 0.786	3.230e-03 0.790	2.141e-04 0.793	1.35e-04 0.797	3.540e-04 0.799	1.572e-04
2^{-12}	7.996e-02 0.743	4.778e-02 0.772	2.797e-02 0.791	1.616e-02 0.801	9.278e-03 0.820	5.256e-03
2^{-14}	8.020e-02 0.742	4.796e-02 0.765	2.821e-02 0.801	1.619e-02 0.804	9.278e-03 0.820	5.256e-03
...
2^{-18}	8.008e-02 0.736	4.806e-02 0.760	2.838e-02 0.798	1.632e-02 0.815	9.278e-03 0.820	5.255e-03
$E^{N,M}$	8.020e-02	5.263e-02	2.838e-02	1.670e-02	9.579e-03	5.411e-03
$P^{N,M}$	0.607	0.891	0.765	0.801	0.824	

This work can be extended to explore the extension of the numerical method to higher-order accuracy. Consider using higher-order finite difference schemes or other numerical techniques, such as spectral methods or finite element methods, to improve the overall accuracy of the solution. Conduct a detailed analysis of the stability and convergence properties of the method. Provide theoretical insights into the behavior of the numerical solution, especially in the presence of singular perturbations and discontinuities. Apply the developed numerical method to real-world problems in science and engineering. Consider problems with physical relevance, such as environmental transport phenomena or heat conduction in materials with abrupt changes.

References

- [1] L. BOBISUD, Parabolic Equations With A Small Parameter And Discontinuous Data, Journal Of Mathematical Analysis And Applications, 26 (1969), Pp. 208–220.
- [2] C. CLAVERO, J. GRACIA, AND J. JORGE, High-Order Numerical Methods For One-Dimensional Parabolic Singularly Perturbed Problems With Regular Layers, Numerical Methods For Partial Differential Equations: An International Journal, 21 (2005), Pp. 149–169.
- [3] C. CLAVERO, J. L. GRACIA, AND F. LISBONA, High Order Methods On Shishkin Meshes For Singular Perturbation Problems Of Convection–Diffusion Type, Numerical Algorithms, 22 (1999), Pp. 73–97.
- [4] C. CLAVERO, J. L. GRACIA, G. I. SHISHKIN, AND L. P. SHISHKINA, An Efficient Numerical Scheme For 1d Parabolic Singularly Perturbed Problems With An Interior And Boundary Layers, Journal Of Computational And Applied Mathematics, 318 (2017), Pp. 634–645.
- [5] C. Clavero, J. Jorge, and F. Lisbona, A uniformly convergent scheme on a nonuniform mesh for convection–diffusion parabolic problems, Journal of Computational and Applied Mathematics, 154 (2003), pp. 415–429.
- [6] E. P. Doolan, J. J. Miller, and W. H. Schilders, Uniform numerical methods for problems with initial and boundary layers, Boole Press, 1980.
- [7] R. K. Dunne, E. O’Riordan, and G. I. Shishkin, A fitted mesh method for a class of singularly perturbed parabolic problems with a boundary turning point, Computational Methods in Applied Mathematics, 3 (2003), pp. 361–372.
- [8] P. Farrell, A. Hegarty, J. Miller, E. O’Riordan, and G. Shishkin, Singularly perturbed convection–diffusion problems with boundary and weak interior layers, Journal of Computational and Applied Mathematics, 166 (2004), pp. 133–151.
- [9] P. Farrell, A. Hegarty, J. M. Miller, E. O’Riordan, and G. I. Shishkin, Robust computational techniques for boundary layers, CRC Press, 2000.
- [10] J. Gracia and E. O’Riordan, A singularly perturbed convection–diffusion problem with a moving interior layer, Int. J. Numer.

- Anal. Model, 9 (2012), pp. 823–843.
- [11] J. Gracia and E. O’Riordan, Numerical approximation of solution derivatives of singularly perturbed parabolic problems of convection-diffusion type, *Mathematics of Computation*, 85 (2016), pp. 581–599.
- [12] J. L. Gracia and E. O’Riordan, Parameter-uniform approximations for a singularly perturbed convection-diffusion problem with a discontinuous initial condition, *Applied Numerical Mathematics*, 162 (2021), pp. 106–123.
- [13] J. L. Gracia and E. O’Riordan, Singularly perturbed reaction–diffusion problems with discontinuities in the initial and/or the boundary data, *Journal of Computational and Applied Mathematics*, 370 (2020), p. 112638.
- [14] J. L. Gracia and E. O’Riordan, Numerical approximations to a singularly perturbed convection-diffusion problem with a discontinuous initial condition, *Numerical Algorithms*, 88 (2021), pp. 1851–1873.
- [15] P. Hemker and G. Shishkin, Discrete approximation of singularly perturbed parabolic pdes with a discontinuous initial condition, in *Bail VI Proceedings*, 1994, pp. 3–4.
- [16] T. Linß, An upwind difference scheme on a novel shishkin-type mesh for a linear convection– diffusion problem, *Journal of computational and applied mathematics*, 110 (1999), pp. 93–104.
- [17] J. Miller, E. O’Riordan, G. Shishkin, and R. B. Kellogg, Fitted numerical methods for singular perturbation problems, *SIAM Review*, 39 (1997), pp. 535–537.
- [18] J. Miller, E. O’Riordan, G. Shishkin, and L. Shishkina, Fitted mesh methods for problems with parabolic boundary layers, in *Mathematical Proceedings of the Royal Irish Academy*, JSTOR, 1998, pp. 173–190.
- [19] J. J. Miller, E. O’riordan, and G. I. Shishkin, Fitted numerical methods for singular perturbation problems: error estimates in the maximum norm for linear problems in one and two dimensions, *World scientific*, 1996.
- [20] E. O’Riordan and G. Shishkin, Singularly perturbed parabolic problems with non-smooth data, *Journal of computational and applied mathematics*, 166 (2004), pp. 233–245.
- [21] E. O’Riordan, M. Pickett, and G. Shishkin, Parameter-uniform finite difference schemes for singularly perturbed parabolic diffusion-convection-reaction problems, *Mathematics of Computation*, 75 (2006), pp. 1135–1154.
- [22] H.-G. Roos, M. Stynes, and L. Tobiska, *Robust numerical methods for singularly perturbed differential equations: convection-diffusion-reaction and flow problems*, vol. 24, Springer Science & Business Media, 2008.
- [23] T. Linß, *Layer-adapted meshes for reaction-convection-diffusion problems*, Springer, 2009.
- [24] G. Shishkin, Robust novel high-order accurate numerical methods for singularly perturbed convection-diffusion problems, *Mathematical Modelling and Analysis*, 10 (2005), pp. 393–412.
- [25] G. I. Shishkin, Grid approximation of singularly perturbed parabolic convection-diffusion equations with a piecewise-smooth initial condition, *Zhurnal Vychislitel’noi Matematiki i Matematicheskoi Fiziki*, 46 (2006), pp. 52–76.
- [26] D. S. Sheiso, Approximation of functions using fourier series and its application to the solution of partial differential equations, *Science Journal of Applied Mathematics and Statistics*, 10 (2022), pp. 57–84.
- [27] N. S. Yadav and K. Mukherjee, On ϵ -uniform higher order accuracy of new efficient numerical method and its extrapolation for singularly perturbed parabolic problems with boundary layer, *International Journal of Applied and Computational Mathematics*, 7 (2021), p. 72.